Supporting Information

Photo-relaxation induced by
water-chromophore electron transfer

Mario Barbatti

Table of Contents

1   Movies

Two movie files are provided as Supporting Information. They look like the snapshot below (Fig. S1). Each file shows one single trajectory either for 9H- or 7H-adenine. The graph in the lower-left corner shows the potential energies during the dynamics. A black dot marks the current state of the molecule every time step. The potential energy of the unoccupied states are computed for the same geometry and shown in the graph.
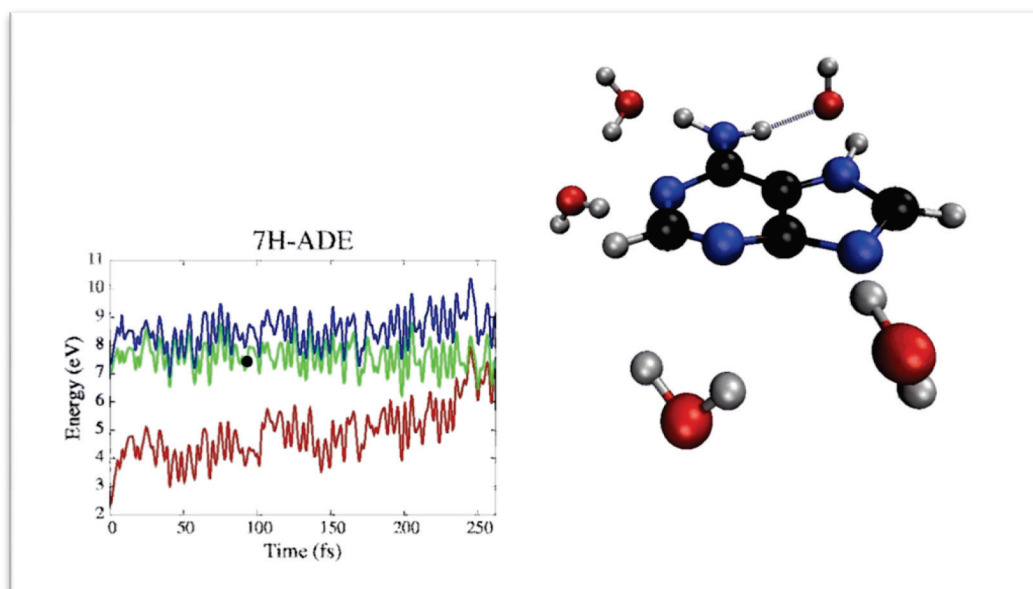

Fig. S1. Snapshot of one of the movies provides as supporting information.

2　Computational Methods

Ab-initio algebraic diagrammatic construction to the second order [ADC(2)][1] was used to simulate the nonadiabatic dynamics of 9H and 7H tautomers of adenine in small water clusters. The ADC(2) method, which was originally derived using diagrammatic perturbation theory,[2] may be expressed by the symmetric Jacobian $\mathbf{A}^{ADC(2)} = \frac{1}{2}(\mathbf{A}^{CIS(D\infty)} + \mathbf{A}^{CIS(D\infty)\dagger})$, where $\mathbf{A}^{CIS(D\infty)}$ is the Jacobian of the CIS(D_∞) coupled-custer approximation.[1] Excited-state energies of either of these approximations correspond to the eigenvalues of the Jacobian, while the contribution of each determinant to the excitation is associated to the eigenvectors.

Adenine-water clusters were optimized in the ground state with the Møller-Plesset perturbation theory to the second order (MP2). aug-cc-pVDZ and cc-pVDZ basis sets were assigned to N and C atoms, respectively.[3] SVP basis set[4] was assigned to O and H atoms. The nuclear ensemble method[5] with 500 points and 5 excited states was used to simulate the absorption spectrum, from where initial conditions for dynamics were selected. 50 trajectories for each tautomer with water and in the gas phase were started from the 4.71 ± 0.05 eV (~263 nm) spectral window, summing to a total of 200 trajectories. For each of the four systems the number of points in the spectral window and the number of trajectories initiated in each state are given in Table S1.

Table S1　　　Number of points in the spectral window and number of trajectories initiated in each state for the four sets of simulations.

			S_1	S_2	S_3-S_6
7H-Ade	Water	Spectrum	51	3	0
		Trajectories	47	3	0
9H-Ade	Water	Spectrum	60	14	0
		Trajectories	41	9	0
7H-Ade	Gas	Spectrum	49	50	0
		Trajectories	25	25	0
9H-Ade	Gas	Spectrum	38	20	0
		Trajectories	33	17	0

Nonadiabatic effects between excited states were taken into account via fewest-switches surface hooping[6] with decoherence corrections (α = 0.1 hartree).[7] Nonadiabatic couplings were computed with the method described in Ref.[8]. With ADC(2), only nonadiabatic transitions between excited states can be computed.[8] Thus, for each trajectory, the time for internal conversion to the ground state was estimated by the first time in which the energy gap between the first excited state and the ground state dropped below 0.15 eV. Trajectories were integrated until this threshold was reached or for a maximum of 1 ps. The time step for integration of classical equations was 0.5 fs. For the quantum

equations, the time step was 0.025 fs, using interpolated quantities between classical steps. All calculations were done with Turbomole[9] and Newton-X[10,11] programs.

The computation of nonadiabatic effects only between excited states deserves some additional explanations. It is a strong restriction, whose validity depends on the properties that are being investigated. In the present work, my aim was to determine the relaxation mechanism of electronically-excited clusters. In this case, nonadiabatic effects between excited states are important, because during the excited-state dynamics, the population flows between different excited states, each one with its own potential-energy landscape. The exact balance of the activation of the several relaxation channels will depend on the proper account of this flow in the different excited states. Usually, the relaxation channel is selected much before nonadiabatic effects between the excited states and the ground state become relevant. This happens because, only after relaxing, the energy gap to the ground state becomes small enough to render nonadiabatic effects important. Therefore, the determination of relaxation mechanisms is a situation where neglecting nonadiabatic effects with the ground state does not affect the final results. If we wanted, however, to investigate isomerization quantum yields, which is a process dependent on how the excited state population is transferred to the ground state, this approximation would not be valid anymore, as nonadiabatic effects with the ground state play a major role.

3   Ground-state geometries and vertical excitations

The optimized clusters are shown in Fig. S2. Distances are given in Angstrom. Their Cartesian coordinates are given at the end of this document.

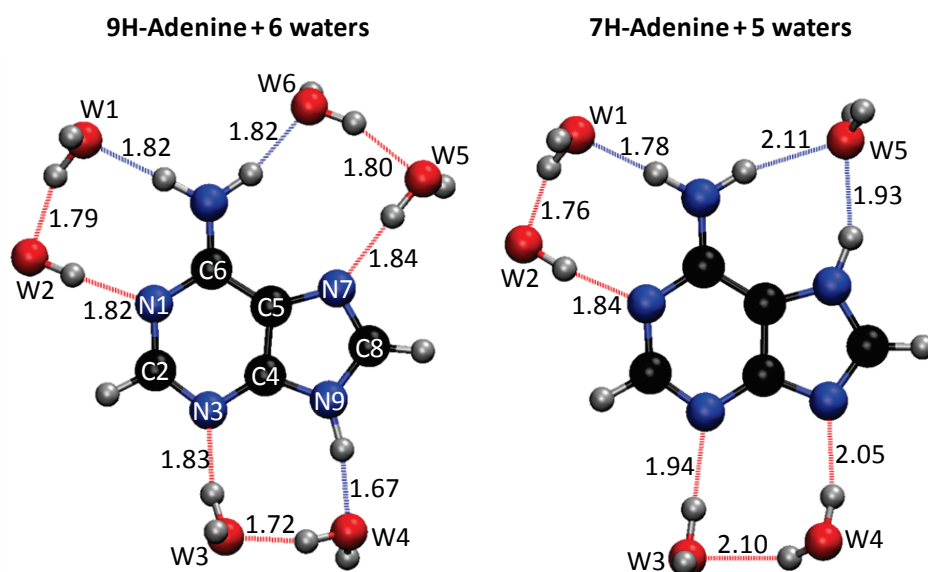**9H-Adenine + 6 waters**   **7H-Adenine + 5 waters**

Fig. S2. Ground-state geometries of the adenine tautomers in water clusters.

The lowest vertical excitation energies and oscillator strengths into singlet states are given in Table S2.

Table S2   Vertical excitation energies, oscillator strengths and state characters.

Ade	Phase	ΔE (eV)	f	State	Phase	ΔE (eV)	f	State
7H	Water	4.85	0.216	$\pi\pi^*$	Gas	4.83	0.014	$n\pi^*$
		5.30	0.007	$n\pi^*$		4.96	0.120	$\pi\pi^*$
		5.38	0.054	$\pi\pi^*$		5.51	0.003	$n\pi^*$
		5.80	0.000	$n\pi^*$		5.54	0.015	π-Ryd
		5.92	0.012	π-Ryd		5.61	0.067	$\pi\pi^*$
		6.16	0.008	$n\pi^*$		5.85	0.003	$n\pi^*$
9H	Water	4.95	0.328	$\pi\pi^*$	Gas	5.08	0.012	$n\pi^*$
		5.10	0.040	$\pi\pi^*$		5.19	0.088	$\pi\pi^*$
		5.47	0.001	$n\pi^*$		5.23	0.203	$\pi\pi^*$
		6.06	0.002	$n\pi^*$		5.72	0.002	$n\pi^*$
		6.22	0.359	$\pi\pi^*$		6.12	0.011	π-Ryd
		6.27	0.070	π-Ryd		6.16	0.002	$n\pi^*$

4 Absorption spectra

Fig. S3 shows the absorption spectra of adenine in the gas phase (vapor) and in water. The solid curves are the results of the simulations. They are weighted sums of 9H-adenine (80%) and 7H-adenine (20%).[12] The dashed curves are experimental results in the gas phase[13] and in water.[14]

The gas-phase simulation is in excellent agreement with the experiment in the low energy region of the spectrum, although it clearly misses states in the high-energy region. For adenine in water, the simulated height and the band width are well described, but the band itself is somewhat red-shifted in relation to the experiment. This difference may be attributed to the modeling, which includes only small water clusters, rather than full water solvation.

These results are included here only for general information. The deviation between the experiment and theory for adenine in water does not have any additional implications for the results discussed in the paper, which should be understood in the context of clusters, not full solvation.
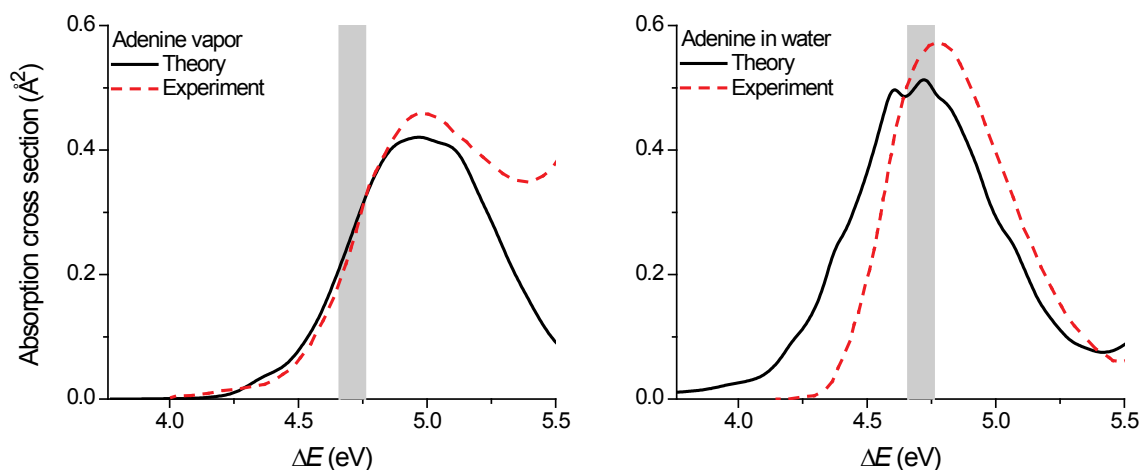

Fig. S3. Simulated and experimental absorption cross section of adenine in the gas phase and in water. Initial conditions for dynamics were sampled from the shaded area.

5   Fate of individual trajectories

Table S3   Results for each simulated trajectory. NSTATDYN is the initial state. t is the final time step, either when the S_1-S_0 energy gap drops below 0.15 eV or 1000 fs is reached. Whn the energy threshold is reached, the reaction path is indicated as WeT – water electron transfer; C2 (puckering); C6 (puckering); PT – water-adenine proton transfer; r-diss – ring dissociation; N7H – N7-H stretching.

| | nH-ADE in Water | | | | | | | | | | | | nH-ADE in Gas | | | | | | | | | | | | |
| | 7H | | | | | | 9H | | | | | | 7H | | | | | | 9H | | | | | | |
NSTATDYN / TRAJ	**2**	t (fs)		**3**	t (fs)		**2**	t (fs)		**3**	t (fs)		**2**	t (fs)		**3**	t (fs)		**2**	t (fs)		**3**	t (fs)	
1	1	259	WeT	1	1000	-	1	157.5	C2	1	145.5	C2	1	1000	-	1	594.5	C6	1	1000	-	1	1000	-
2	2	862.5	WeT	2	251	WeT	2	231.5	C2	2	600	C2	2	815	C6	2	1000	-	2	149	C2	2	1000	-
3	3	172	WeT	3	142.5	C2	3	65.5	C6	3	234	C2	3	1000	-	3	927	C6	3	1000	-	3	500.5	C2
4	4	262	WeT				4	373.5	C2	4	461	C6	4	1000	-	4	856.5	C6	4	702	C6	4	54.5	C2
5	5	1000	-				5	122	C2	5	214.5	C2	5	1000	-	5	1000	-	5	1000	-	5	69	C2
6	6	174.5	WeT				6	97.5	C2	6	367	PT	6	271.5	r-diss	6	1000	-	6	624.5	C6	6	670	C6
7	7	222	C2				7	148.5	C2	7	120.5	C2	7	1000	-	7	1000	-	7	1000	-	7	1000	-
8	8	277.5	WeT				8	431.5	C2	8	176.5	C2	8	1000	-	8	684	r-diss	8	1000	-	8	1000	-
9	9	119.5	C2				9	62	C2	9	474	C2	9	930.5	C6	9	950	C6	9	788.5	C6	9	258	C6
10	10	420	WeT				10	340	C2				10	1000	-	10	1000	-	10	574	C2	10	1000	-
11	11	489.5	WeT				11	207	C2				11	470.5	C6	11	1000	-	11	1000	-	11	1000	-
12	12	1000	-				12	307	C2				12	1000	-	12	76	r-diss	12	1000	-	12	1000	-
13	13	379.5	WeT				13	399.5	C2				13	1000	-	13	1000	-	13	715	C6	13	1000	-
14	14	508	WeT				14	84	C2				14	727	C6	14	1000	-	14	428.5	C6	14	527	C6
15	15	1000	-				15	19	PT				15	24	N7H	15	1000	-	15	1000	-	15	798	C2
16	16	497	WeT				16	158	C2				16	330.5	C6	16	1000	-	16	1000	-	16	334	C2
17	17	698.5	WeT				17	345.5	C2				17	1000	-	17	1000	-	17	184	C2	17	1000	-
18	18	1000	-				18	218	C2				18	1000	-	18	1000	-	18	872.5	C6			
19	19	253	WeT				19	168.5	C2				19	551	C2	19	985	C6	19	800.5	C2			
20	20	253.5	WeT				20	290.5	C2				20	798.5	C6	20	1000	-	20	1000	-			
21	21	384.5	C2 (PT)				21	133.5	C2				21	58.5	N7H	21	1000	-	21	1000	-			
22	22	214.5	C6				22	112.5	C2				22	1000	-	22	1000	-	22	885.5	C6			
23	23	347	WeT				23	70.5	C2				23	1000	-	23	1000	-	23	1000	-			
24	24	1000	-				24	167	C2				24	1000	-	24	1000	-	24	1000	-			
25	25	194	WeT				25	116	C2				25	1000	-	25	779.5	C6	25	503.5	C6			
26	26	609.5	WeT				26	198	C2										26	611.5	C2			
27	27	317	C2				27	300.5	C2										27	1000	-			
28	28	347	WeT				28	254.5	C2										28	902.5	C6			
29	29	1000	-				29	153	C2										29	1000	-			
30	30	1000	-				30	221.5	C2										30	744.5	C6			
31	31	516.5	WeT				31	106	C2										31	1000	-			
32	32	1000	-				32	199.5	C2										32	581.5	C6			
33	33	731.5	WeT				33	392.5	C2										33	1000	-			
34	34	1000	-				34	301	C2															
35	35	218.5	WeT				35	68.5	C2															
36	36	1000	-				36	25.5	PT															
37	37	257.5	WeT				37	275.5	C2															
38	38	1000	-				38	112.5	C2															
39	39	1000	-				39	147	C2															
40	40	593.5	WeT				40	200.5	C2															
41	41	219.5	WeT				41	449.5	C2															
42	42	1000	-																					
43	43	1000	-																					
44	44	632.5	WeT																					
45	45	278	WeT																					
46	46	242	WeT																					
47	47	646.5	WeT																					

6   Deactivation channels and statistical errors

Table S4 shows the probability of occurrence of the several relaxation mechanisms. These mechanisms are: C2 (puckering); C6 (puckering); WeT – water electron transfer; R-Diss – ring dissociation; H-Diss – N-H stretching. PT – water-adenine proton transfer; NR – not relaxed within 1000 ps. Margins of errors for the relaxation probabilities were computed according to[15]

$$\varepsilon = Z\sqrt{\frac{p(1-p)}{N}} ,$$

where p is the probability, N is the number of trajectories and $Z = 1.6449$ for a 90% confidence interval.

Table S4   Distribution of probabilities among all reaction channels.

Ade		C2	C6	WeT	R-Diss	H-Diss	PT	NR
				Mechanism Probability				
7H	Water	0.10±0.07	0.02±0.03	0.58±0.11	0	0	0	0.30±0.11
9H	Water	0.90±0.07	0.04±0.05	0	0	0	0.06±0.06	0
7H	Gas	0.02±0.03	0.24±0.10	-	0.06±0.06	0.04±0.05	-	0.64±0.11
9H	Gas	0.20±0.09	0.28±0.10	-	0	0	-	0.52±0.12
9H[a]	Gas	0.28±0.07	0.21±0.07	-	0	0.04±0.03	-	0.47±0.08

[a] Result of Ref.[8] with ADC(2)/aug-cc-pVDZ.

7   Population fitting and lifetimes

Lifetime was obtained by plotting the distribution of relaxation times to the ground state and then fitting this distribution with the function

$$f\left(t\right) = f_0 + \left(1 - f_0\right)\exp\left(-\left(t / \tau_l\right)^2\right).$$

The data was fitted between 0 and 1000 fs. f_0 was kept fixed in zero for all cases, except 7H-Ade+5W, where a clear asymptotic level could be distinguished within the simulation time. The data for the four sets of simulations and the respective fittings are shown in Fig. S4.
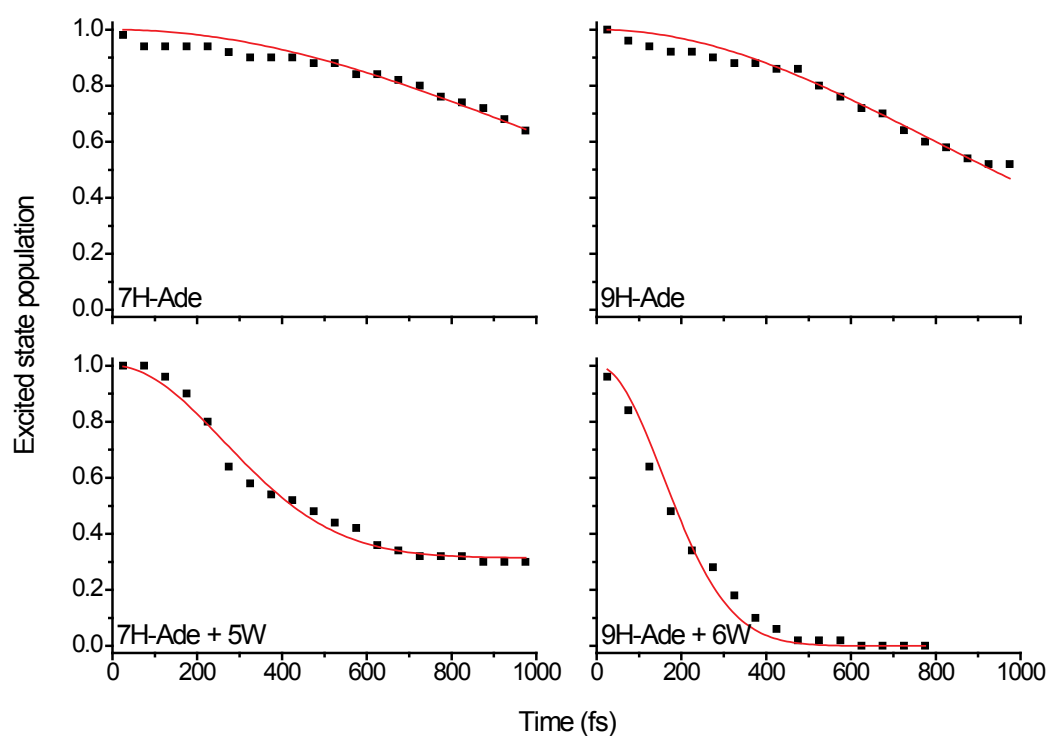
Fig. S4. Excited-state population as a function of time for the four sets of simulated data.

8   State analysis of a representative trajectory

Fig. S5 illustrates the time evolution for one single trajectory of 7H-adenine in water cluster. It features the main elements shared by all trajectories following the water-chromophore electron transfer pathway. This particular trajectory started in the first excited state and did not hop to the second during the simulations. The graph shows the energy gap between the ground and the first excited state. The data was smoothed over 40 fs to reduce the fast energy oscillations due to hydrogen stretching vibrations.

Initially, the $\pi\pi^*$ state is populated. A very fast relaxation (< 50 fs) of the rings leads to a state mixing between $\pi\pi^*$ and $n\pi^*$. Similar relaxation is observed also in the gas phase, as well as for 9H-adenine. The system remain in this mixed $\pi\pi^*+n\pi^*$ state for most of time. The n orbital is at beginning mainly localized at the pyrimidine ring (see orbital at time 0 in Fig. S5). Gradually, there is a density transfer to the n orbital at the water molecule near N3 (see the sequence of orbitals in Fig. S5). At the end of the trajectory, the π contribution disappears and the n orbital has equal contributions from n_O and n_N.
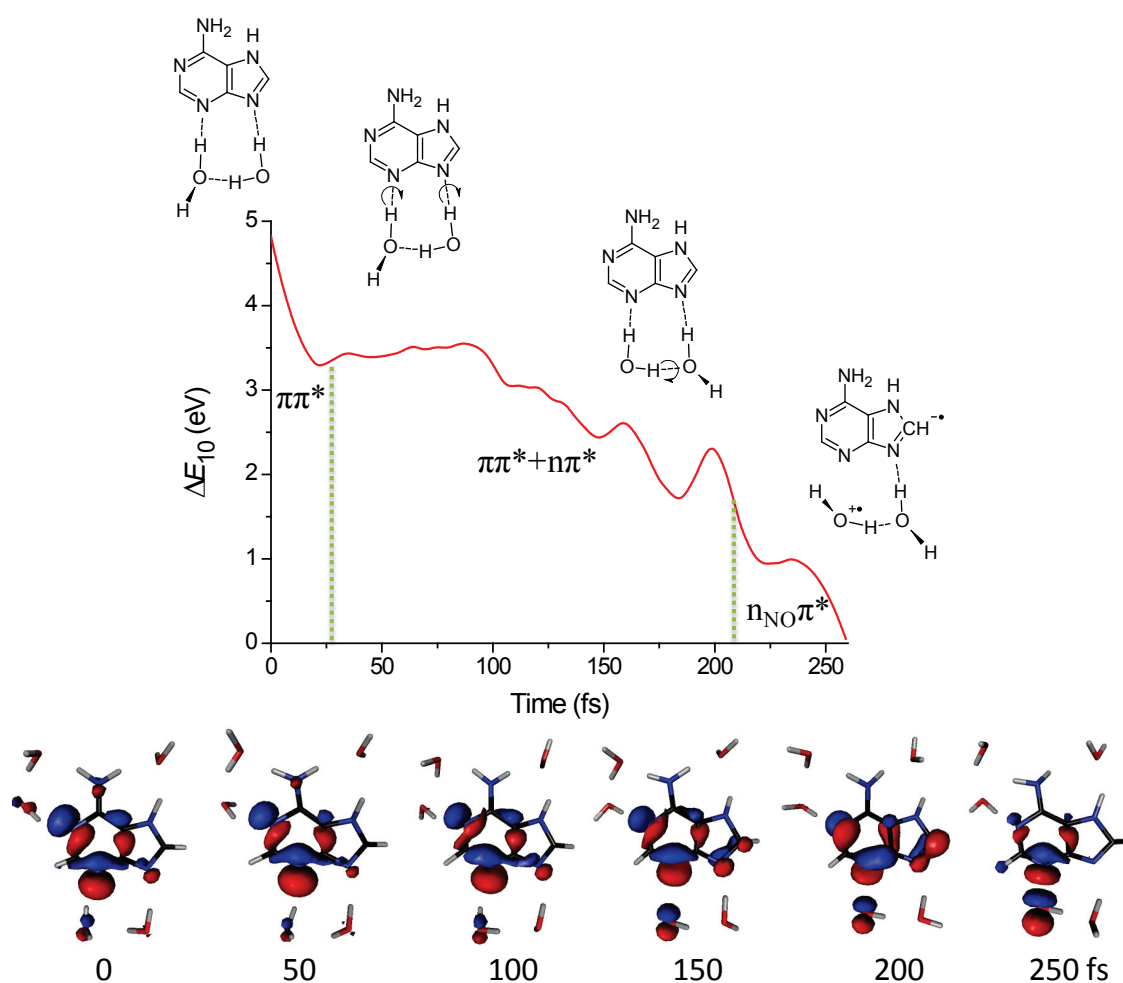

Fig. S5. Time evolution of a single trajectory of 7H-adenine in water. The energy gap was smoothed over 40 fs windows.

A fundamental feature of the water-chromophore electron transfer pathway is the rearrangement of the solvent molecules. It happens in two steps. First, there is a simultaneous twist of the water molecules near N3 and N7, leading to a new hydrogen bond pattern:
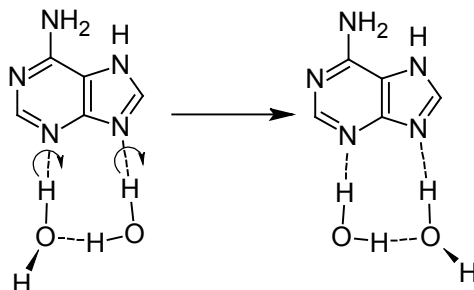
Then, a new twist around the OHO axis breaks the H-bond to N3 and tunes the S_1-S_0 intersection:
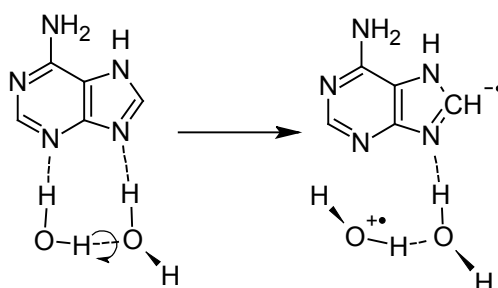
The simulation of this trajectory was extended up to 400 fs (141 fs more) to gain some insight on the motion near the crossing seam (see Fig. S6). During this additional time, the complex remained in the electron-transfer state with the 7H-adenine essentially planar and slightly pyrimidalized at C8. This shows that this region of the potential energy surface is a stable minimum in the S_1 state. In the first 10 fs, the energy gap reduced from 0.15 eV (the original threshold) to -0.73 eV. The negative value means that the excited state is lower in energy than the ground state. Negative excitation energies are one of the problems of ADC(2) when computed near the crossing seam, but in this case, it is also strong evidence that the seam is in fact in that region. Within 20 fs of the complementary time, the energy gap increased again to 0.15 eV. By 100 fs, it increased to about 2 eV and then reduced back towards the crossing seam, reaching 0.38 eV at 400 fs. This behavior may indicate that the molecule is slowly vibrating around the minimum where the crossing seam lays with a period of approximately 280 fs (120 cm^{-1}).

Albeit all methodological caveats of propagating ADC(2) dynamics near the seam for such long period, these results indicate that 1) there is a minimum on the S_1 surface with water-chromophore electron-transfer character, that 2) this minimum is near a crossing seam with the ground state, and 3) that the molecule moves near this seam for few tens of femtoseconds.
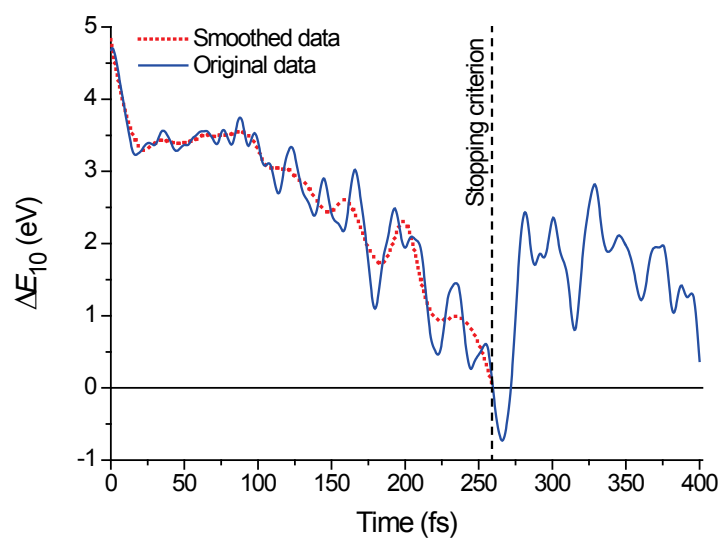
Fig. S6. S_1-S_0 energy gap along a selected trajectory extended for 141 fs after the stopping criterion was achieved.

9   Comparison to a fully-correlated method

To check the possibility that the water-chromophore electron transfer pathway is not an artifact of the ADC(2) method, the complete active space perturbation theory to the second order (CASPT2) was used to cross-check the results. For the representative trajectory discussed in the previous section, single-point CASPT2 calculations were done for the geometries at 0, 50, 100, 150, 200, and 259 fs.

The CASPT2 and multi-state (MS) CASPT2 calculations were based on an active space composed of 14 electrons in 10 orbitals. For all snapshots, this space consisted of 2 n, 5 π, and 3 π* orbitals. A total of 4 electronic states were included in the state-averaging procedure. Calculations were performed including the IPEA shift[16] (0.25 au) and a real level shift of 0.1 au. The 6-31G* basis set was adopted for all atoms. The CASPT2 calculations were performed with the Molcas 7.6 program.[17]

Fig. S7 shows the S_1-S_0 energy gaps along the trajectory. Both single- and multi-state CASPT2 results are in average 0.5 eV above the ADC(2) data. The fact that these sets of data are parallel to each other is a positive indication of the good quality of the ADC(2) dynamics. At the end of the trajectory, the energy gap is about 0.7 eV at CASPT2 against 0.11 eV at ADC(2). This divergence was expected as the tuning of the crossing-seam geometry is very sensible to the computational method. In any case, energy gaps smaller than 1 eV usually indicate the proximity to the crossing seam.
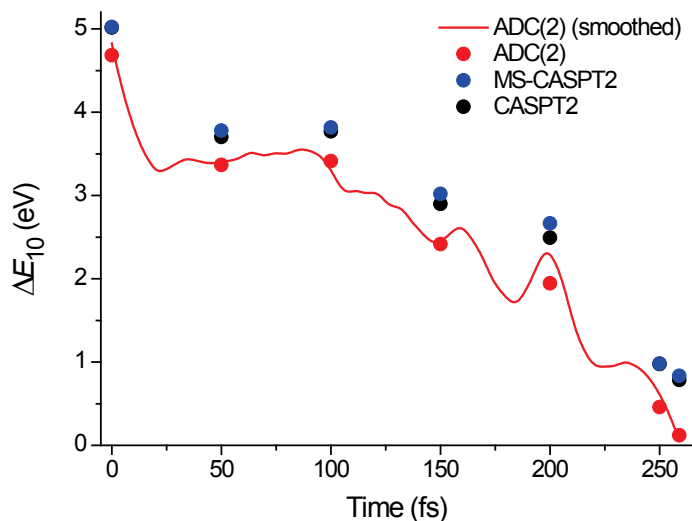

Fig. S7. S_1-S_0 energy gap along a selected trajectory. The solid line is the ADC(2) energy gap smoothed over 40 fs windows. Red dots indicate the ADC(2) raw results. Blue and black dots indicate respectively MS-CASPT2 and CASPT2 results.

Besides energy, it is important to check the character of the states as well. As shown in Table S5, there is an excellent correspondence between those characters computed with both methods. It is gratifying

to see that even the mixing between the $\pi\pi^*$ and the $n\pi^*$ states is in good agreement between the two methods.

Table S5   Main configurations contributing to the S_1 state along a selected trajectory.

Methods	0	50	100	150	200	250	259
				Time (fs)			
ADC(2)	$\pi\pi^*$	$\pi\pi^*+n\pi^*$	$\pi\pi^*$	$\pi\pi^*+n\pi^*$	$n\pi^*+\pi\pi^*$	n_{NO}-π^*	n_{NO}-π^*
CASPT2	$\pi\pi^*$	$\pi\pi^*+n\pi^*$	$\pi\pi^*$	$\pi\pi^*+n\pi^*$	$\pi\pi^*+n\pi^*$	n_{NO}-π^*	n_{NO}-π^*

At the end of the trajectory (t > 200 fs), the S_1 state is dominated by the n_{NO}-π^* transition, which characterizes the electron-transfer state. The n_{NO} and the π^* Hartree-Fock orbitals used in the ADC(2) calculations and the CASSCF orbitals used in the CASPT2 calculations computed for the 259-fs geometry are shown in Fig. S8.
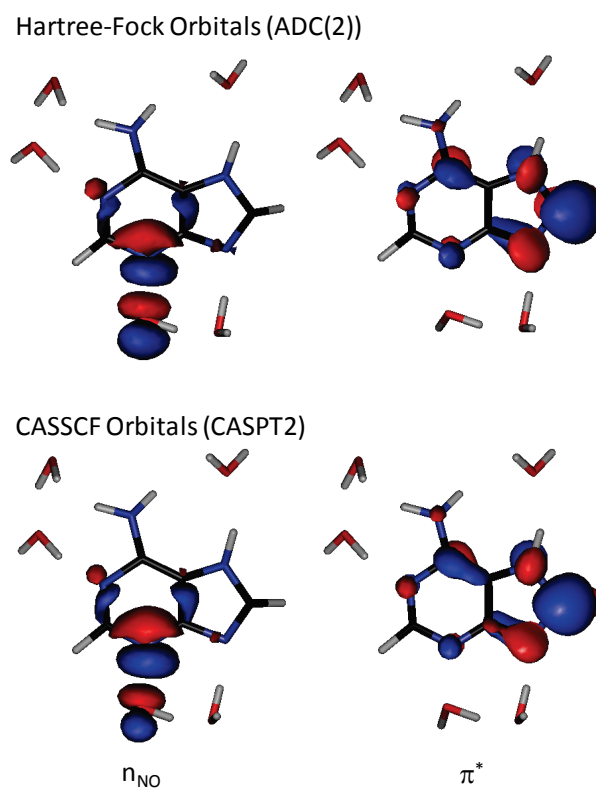

Hartree-Fock Orbitals (ADC(2))

CASSCF Orbitals (CASPT2)

n_{NO} π^*

Fig. S8. Singly-occupied molecular orbitals at 259 fs.

10 Charge-transfer analysis

The S_1-S_0 intersection structure for all trajectories for 7H-adenine in water was analyzed in terms of natural population of the S_1 density. The distribution of charge in the 7H-adenine at these points is shown in Fig. S9. It indicates that 0.4 ± 0.1 electron is transferred from water to 7H-adenine.
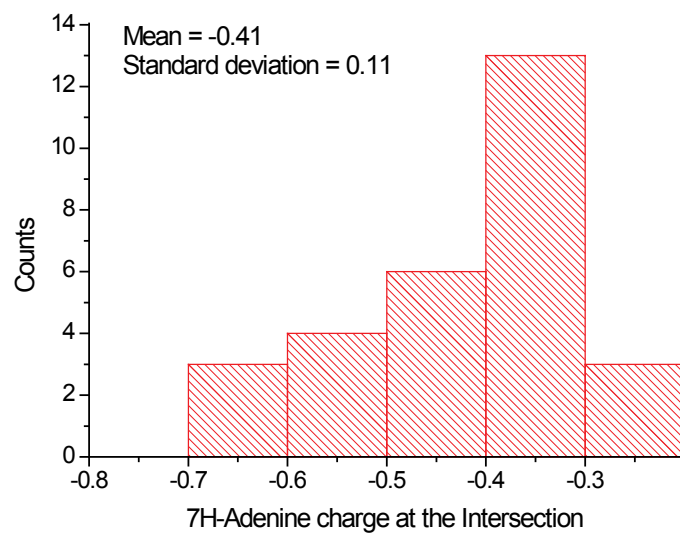

Fig. S9. Distribution of charge in 7H-Adenine at the intersection point.

11   Intersection characterization (geometry, dipole, IP)

Fig. S10 shows some key geometric parameters in the structure of the S_1-S_0 intersection. This structure is the same shown in Fig. 4 of the paper. Its Cartesian coordinates are provided later in this document. Still for this structure, the dipole moment of the first excited state is given in Table S6. Considering all trajectories following the electron-transfer pathway (WeT), the mean S_1 dipole at the crossing point is $<|\mathbf{d}_{S1}|> = 1.3 \pm 0.5$ au (3.3 ± 1.3 D). For comparison, Table S6 brings the dipole moment for a C2-pukcering intersection occurring in one of the 7H-adenine trajectories (Cartesian coordinates are also provided). The dipole moment is substantially bigger for the C2 intersection than for the WeT intersection.
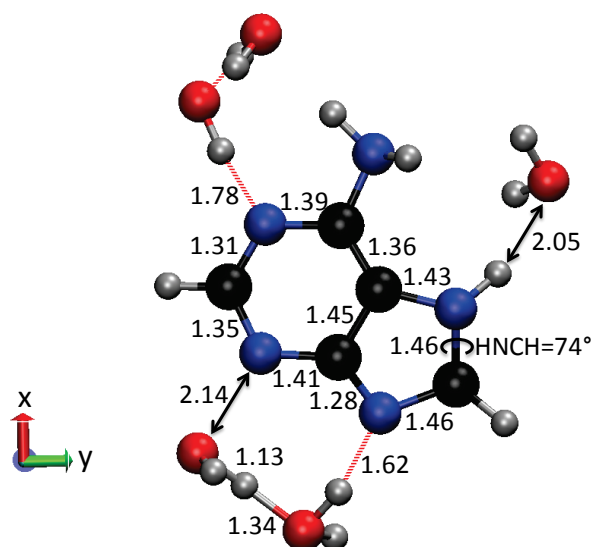

Fig. S10.   Key geometric parameters at the S_1-S_0 intersection (Å, degrees).

Table S6   Dipole moment of the S_1 state at the crossing points of two trajectories ending at the water-chromophore electron-transfer intersection (WeT X) and at the C2-puckered crossing (C2 X) for 7H-adenine in water cluster.

	d_x (au)	d_y (au)	d_z (au)	$|\mathbf{d}|$ (au)
WeT X	-1.33	-0.53	0.70	1.59
C2 X	3.07	3.44	-0.27	4.62

The low-energy vertical spectrum of the neutral and cation is given in Table S7 for the same C2 and WeT intersections and also for the S_0 minimum. Ionization from the S_1 state requires at least 5.05 eV at the S_0 minimum, 7.94 eV from the C2 intersection, and 7.27 eV from the WeT intersection.

These differences on the S_1 dipole moment and ionization potential may be explored for experimental characterization of the WeT pathway in 7H-adenine through time-resolved photoelectron spectroscopy.

Table S7　　　Energies of the lowest singlet (neutral) and doublet (cation) states near the ground state minimum, the C2-puckered crossing (C2 X), and the water-chromophore electron-transfer intersection (WeT X) for 7H-adenine in water cluster.

State	ΔE (eV)		
	S_0 min	C2 X	WeT X
S_0	0.00	0.00	0.00
S_1	4.84	0.02	0.12
D_1	9.89	7.96	7.39
D_2	12.66	8.68	10.11

12   Additional references

(1)   Hättig, C. *Adv. Quantum Chem.* **2005**, *50*, 37-60.
(2)   Schirmer, J. *Phys. Rev. A* **1982**, *26*, 2395-2416.
(3)   Dunning, T. H. *J. Chem. Phys.* **1989**, *90*, 1007-1023.
(4)   Weigend, F.; Ahlrichs, R. *Phys. Chem. Chem. Phys.* **2005**, *7*, 3297-3305.
(5)   Crespo-Otero, R.; Barbatti, M. *Theor. Chem. Acc.* **2012**, *131*, 1237.
(6)   Tully, J. C. *J. Chem. Phys.* **1990**, *93*, 1061-1071.
(7)   Granucci, G.; Persico, M. *J. Chem. Phys.* **2007**, *126*, 134114-134111.
(8)   Plasser, F.; Crespo-Otero, R.; Pederzoli, M.; Pittner, J.; Lischka, H.; Barbatti, M. *J. Chem. Theory Comput.* **2014**, *10*, 1395-1405.
(9)   Ahlrichs, R.; Bär, M.; Häser, M.; Horn, H.; Kölmel, C. *Chem. Phys. Lett.* **1989**, *162*, 165-169.
(10)   Barbatti, M.; Ruckenbauer, M.; Plasser, F.; Pittner, J.; Granucci, G.; Persico, M.; Lischka, H. *WIREs: Comp. Mol. Sci.* **2014**, *4*, 26-33.
(11)   Barbatti, M.; Granucci, G.; Ruckenbauer, M.; Plasser, F.; Crespo-Otero, R.; Pittner, J.; Persico, M.; Lischka, H. *NEWTON-X: a package for Newtonian dynamics close to the crossing seam* **2013**, www.newtonx.org.
(12)   Cohen, B.; Hare, P. M.; Kohler, B. *J. Am. Chem. Soc.* **2003**, *125*, 13594-13601.
(13)   Clark, L. B.; Peschel, G. G.; Tinoco, I. *J. Phys. Chem.* **1965**, *69*, 3615-3618.
(14)   Middleton, C. T.; de La Harpe, K.; Su, C.; Law, Y. K.; Crespo-Hernández, C. E.; Kohler, B. *Annu. Rev. Phys. Chem.* **2009**, *60*, 217-239.
(15)   Devore, J. L. *Probability & Statistics for Engineering and the Sciences*; 8th ed.; Cengage Learning: Stamford, 2012.
(16)   Ghigo, G.; Roos, B. O.; Malmqvist, P.-A. *Chem. Phys. Lett.* **2004**, *396*, 142-149.
(17)   Karlström, G.; Lindh, R.; Malmqvist, P. A.; Roos, B. O.; Ryde, U.; Veryazov, V.; Widmark, P. O.; Cossi, M.; Schimmelpfennig, B.; Neogrady, P.; Seijo, L. *Comp. Mater. Sci.* **2003**, *28*, 222-239.

13 Cartesian coordinates

All geometries are in standard XYZ format in Angstrom.

Ground state 9H-Adenine + 6 Waters

```
N     1.537613     0.976539     2.600768
C     0.618989     0.049460     2.954870
N    -0.219984    -0.639254     2.166610
C    -0.069812    -0.285636     0.863149
C     0.838550     0.659120     0.349117
C     1.705362     1.304195     1.283463
N     0.712479     0.749640    -1.027908
C    -0.256496    -0.132402    -1.320212
N    -0.754662    -0.780434    -0.225633
N     2.649436     2.190444     0.948656
H     0.558775    -0.163114     4.027856
H    -0.621873    -0.336155    -2.326089
H    -1.543669    -1.466212    -0.191063
H     3.297611     2.528049     1.674471
H     2.828273     2.457587    -0.027580
O     2.445540     2.499862     4.771281
H     2.115174     1.937858     4.032536
H     1.763267     3.176066     4.857796
O     3.405056     3.271736    -1.554448
H     3.036579     4.160306    -1.617902
H     3.020823     2.811800    -2.329856
O     1.872272     1.865763    -3.344648
H     1.512111     1.444505    -2.533703
H     1.131894     2.401721    -3.652544
O    -1.582536    -3.052220     2.530298
H    -1.101907    -2.192186     2.553660
H    -0.885021    -3.709920     2.635068
O    -2.734986    -2.588743     0.153282
H    -3.608399    -2.245667     0.377746
H    -2.391054    -2.927575     1.014843
O     4.437892     3.069918     2.991478
H     3.838639     2.998386     3.764433
H     5.111424     2.404181     3.172892
```

Ground state 7H-Adenine + 5 waters

```
N     1.074305     0.525761     1.748682
C     0.248037    -0.492406     2.125957
N    -0.748756    -1.053764     1.437822
C    -0.927177    -0.492724     0.211974
C    -0.123063     0.555710    -0.278300
C     0.925222     1.075324     0.522375
N    -0.599739     0.834906    -1.539191
C    -1.650101    -0.031790    -1.753371
N    -1.882035    -0.845203    -0.725955
N     1.738197     2.085854     0.126183
H     0.436438    -0.891667     3.127796
H    -0.236628     1.548848    -2.171751
H    -2.214425    -0.025919    -2.684859
H     2.593619     2.295834     0.663794
H     1.655267     2.425564    -0.824969
O     2.472360     1.911560     3.759919
H     1.961562     1.369007     3.116983
```

```
H     1.811106     2.505902     4.133295
O    -2.278513    -3.156048     2.726068
H    -1.836483    -2.381813     2.331535
H    -1.687115    -3.868159     2.453474
O    -2.700237    -3.676845    -0.154144
H    -2.499881    -2.783901    -0.468432
H    -2.943782    -3.507631     0.767093
O     4.017353     2.658777     1.670788
H     4.703645     1.981144     1.667744
H     3.579726     2.525558     2.541368
O     0.918434     2.991756    -2.713372
H     0.603747     3.906015    -2.718059
H     1.533235     2.947912    -3.457919
```

WeT S_1-S_0 intersection 7H-Adenine + 5 waters (approximated)

```
N     1.031542     0.507861     1.760390
C     0.297997    -0.484595     2.209691
N    -0.462406    -1.242827     1.391967
C    -0.648864    -0.835312     0.054361
C     0.207485     0.202142    -0.482551
C     0.947549     0.886671     0.426358
N    -0.250395     0.471088    -1.809989
C    -1.527321    -0.228153    -1.850966
N    -1.639459    -1.129147    -0.704100
N     1.663117     2.083630     0.153636
H     0.349317    -0.779157     3.287195
H    -0.293207     1.479482    -2.190810
H    -1.900225    -0.592904    -2.909171
H     2.326798     2.280663     0.915807
H     2.050112     1.838838    -0.733859
O     1.944206     2.252982     3.674485
H     1.441622     1.633817     3.074710
H     1.281507     2.853573     4.136213
O    -1.552109    -2.916905     2.147668
H    -1.159488    -3.567213     1.446564
H    -2.444912    -2.740365     1.481694
O    -3.167745    -2.919028     0.367533
H    -2.598223    -2.339448    -0.203351
H    -4.063449    -2.233652     0.252079
O     4.128045     2.340311     1.992702
H     4.359191     1.323060     1.990429
H     3.326962     2.390689     2.611604
O     0.075504     3.490341    -2.383819
H     0.998085     3.631516    -2.025712
H    -0.473944     3.486023    -1.597370
```

C2-puckered S_1-S_0 intersection in 7H-Adenine + 5 waters (approximated)

```
N    -1.074439    -1.316565     0.174325
C     0.296383    -1.742631     0.511185
N     1.283374    -1.172443    -0.487275
C     1.248486     0.164239    -0.264169
C     0.113396     0.801514     0.291578
C    -1.114223     0.061360     0.308395
N     0.299790     2.179450     0.173784
C     1.556152     2.321914    -0.425533
N     2.090461     1.171492    -0.805098
N    -2.271269     0.697579    -0.015829
```

```
H      0.668398    -2.049193     1.462848
H     -0.441854     2.962335     0.183171
H      1.945034     3.319760    -0.863664
H     -3.074982     0.048881     0.034299
H     -2.300896     1.577651     0.219981
O     -3.186018    -3.059378    -0.704784
H     -2.501293    -2.487520    -0.609405
H     -2.988647    -3.538505    -1.724523
O      3.829994    -2.430437    -0.323801
H      3.005167    -2.132771    -0.545459
H      4.062393    -2.335069     0.686184
O      4.937524     0.097530     0.858865
H      4.049631     0.569676     1.126942
H      4.835729    -0.399144     0.037890
O     -4.444496    -0.956156     0.718971
H     -4.455567    -1.317767     1.627413
H     -4.205379    -1.684617     0.148213
O     -2.216852     3.678306    -0.127366
H     -1.935914     3.917575    -1.048138
H     -2.919624     4.354832     0.081090
```